pattern recognition, multispectral analysis,
image processing, image segmentation

Marcin MICHALAK[1], Karolina NURZYŃSKA[1], Adam ŚWITOŃSKI[1,2]

DETECTION OF HUMAN EYE COMPONENTS ON THE BASIS OF MULTISPECTRAL IMAGING

In this paper the methods for selecting of the most important parts of the human eyes are described. On the basis of the real 21 channel multispectral images the model of finding the lens and the spot are defined. These methods are based on the most popular algorithms of image processing. The approach to veins detection is still undefined but in the article the most important channels are pointed out and the channel difference between eyelash and the veins is also mentioned.

1. INTRODUCTION

Multispectral and hyperspectral imaging becomes more popular method of data analysis. It is due to the fact that bigger number of image spectra is expected to give more information about the object that typical picture in the RGB (three-dimensional) colour space. It is assumed that the increase of the spectra components would provide more information about the object. Multispectral imaging gives also the opportunity to define interesting, from the object properties point of view, spectrum channels (wavelengths). Apart from the medical application, especially the tumor and cancer detection [5, 10, 12], multispectral imaging is successfully applied in geology [1, 6], agriculture [2], or art history [4].

In this article the new approach of analyzing the human eye multispectral images is described. The main aim is to detect the basic eye components on the basis of information stored in different image spectrum. The paper is organized as follows: the next part presents the background of the performed analysis including the hyperspectral image description. Then the processing of the image for the purpose of different eye parts detection is described. The paper ends with a short summary.

2. BACKGROUND

Medicine is one of the fields of multispectral imaging application. Our previous works in this domain focused on the following tasks: detection of tumor tissue regions [12], selection of most important image components for the purpose of tumor tissue [9], nonparametric calibration of multispectral images on the basis of known spectra [7, 8]. The research was conducted on the basis of 21 channel multispectral images obtained from the specialized acquisition device containing the endoscope, liquid crystal tunable filter [3], and the camera. The images are taken with different wavelength from range 410nm to 710nm with the step of 15 nm.

The experiments with an endoscope based device led to the invention of analogical device, strongly dedicated to purpose of ophthalmic imaging. It also consists of the liquid crystal tunable filter (Varispec). The filter is placed after the module of the optical focusing. The remaining part of the spectrum that passes through the filter is captured by a high sensitive monochrome camera (Andor Luca). The camera and the filter are synchronized by the dedicated software. The picture of the acquisition device is presented in Fig. 1. The more detailed information about the device is available in [11].

[1] Silesian University of Technology, ul. Akademicka 16, 44-100 Gliwice, Poland,
email: {Marcin.Michalak, Karolina.Nurzynska, Adam.Switonski}@polsl.pl.
[2] Polish-Japanese Institute of Information Technology, ul. Koszykowa 86, 02-008 Warszawa, Poland.

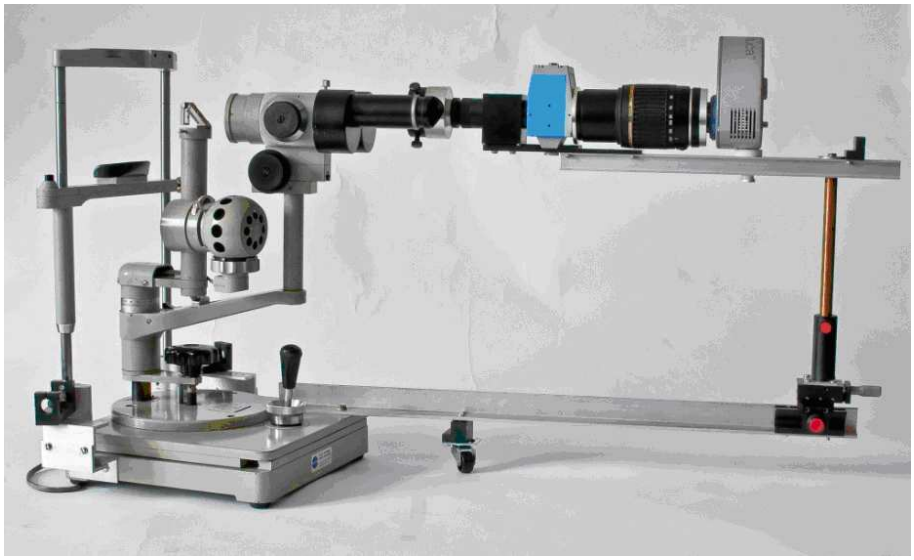

Fig. 1. Acquisition device.

3. MULTISPECTRAL IMAGE PROCESSING

The aim of this research was to design an algorithm which facilitates understanding of multispectral images of an eye. The problem with multispectral data is that the group of images acquired with different spectrum contains all information, although it is impossible to choose one image with all necessary data. Please refer to Fig. 2, where 20 multispectral images out of considered 21 are presented. The first image was omitted due to the lack of space, additionally it was very similar to the one in the top, left corner.

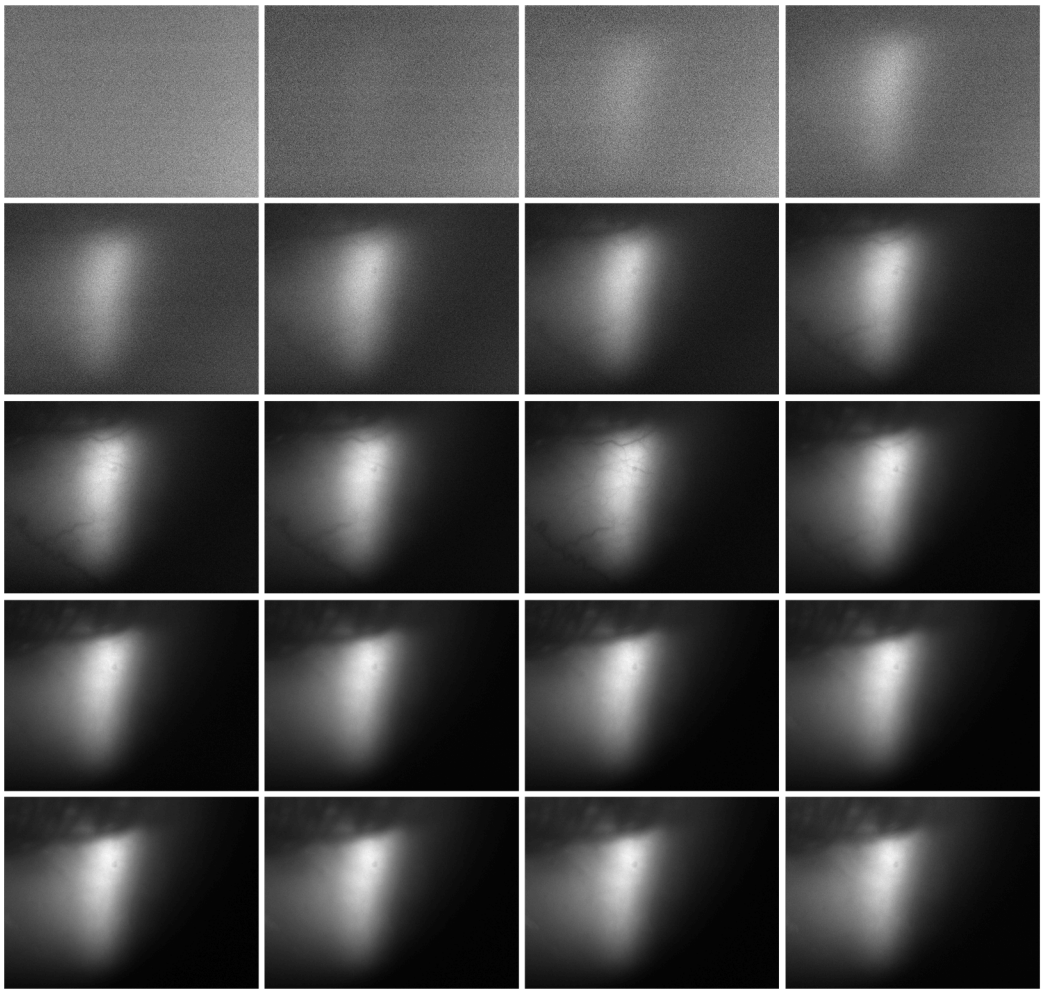

Fig. 2. Images of the human eye taken with different spectrum.

The main objectives of presented work are:

- identify the region of the lens in the image,
- define the region which corresponds to the spot on the lens,
- extract lines which describe the veins, which are noticeable on the lens.

The points of interests are also presented in Fig. 3. Since each of the mentioned problems has different characteristic, it was necessary to design a separate solution. Below the description is given.

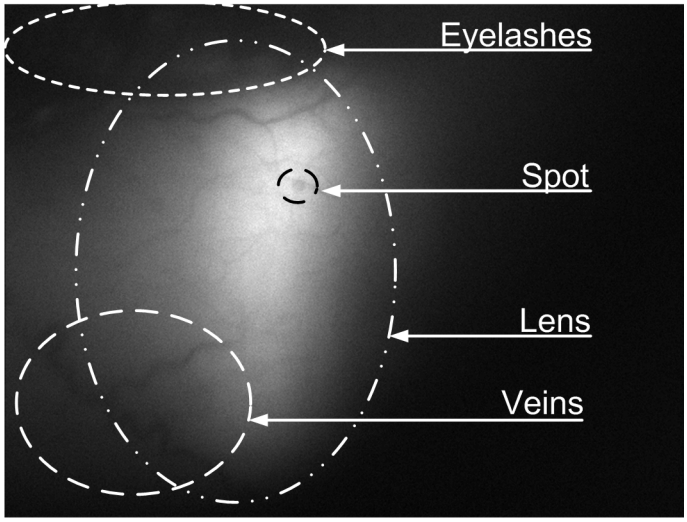

Fig. 3. Exemplary image of the human eye with marked regions of interest.

3.1. LENS DETECTION

The region of the lens in the image is characterized by brighter luminance values in grayscale images. It is visible in many spectra, however its position differs slightly depending on chosen spectrum. Therefore, in order to define more precise lens position and shape it is defined on the basis of average value.

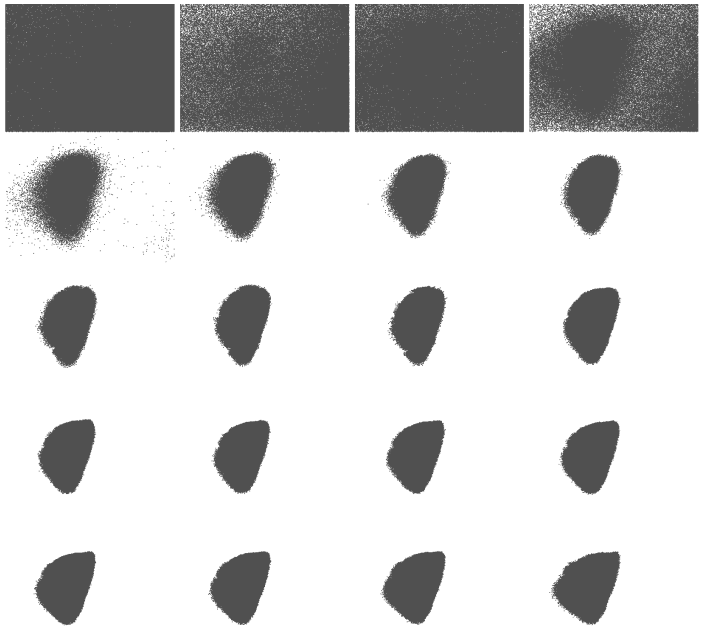

Fig. 4. Mask of lens for multispectral images.

Namely, there are given N=21 images $I(x,y)$ presenting data in each spectrum, where x and y indices the pixel in the image. The image is thresholded to find a mask $M(x,y)$ of the lens. The applied threshold value was equal to 110. Brighter pixels were assumed to describe the object of interest (and assigned value 0 in the mask). Otherwise, darker pixels were treated as background (set value 1 in the mask). Fig. 4. presents masks resulting from thresholding for data given in Fig. 5. Since the lens is not visible on all images, only masks in range 5-21 are considered in averaging. The calculation of final lens shape follows the formula:

$$Lens(x,y) = \begin{cases} 1 & \frac{1}{N-5}\sum_{i=5}^{N} M_i(x,y) < 0.5 \\ 0 & otherwise \end{cases} \quad (1)$$

This algorithm firstly calculates an average mask for images taken for chosen wavelengths, then it thresholds with value 0.5. It corresponds to the assumption that pixel belongs to the lens if it belongs to the object in more than 50% of masks. In this equation value 5 refers to first 5 images, which are excluded from calculation.

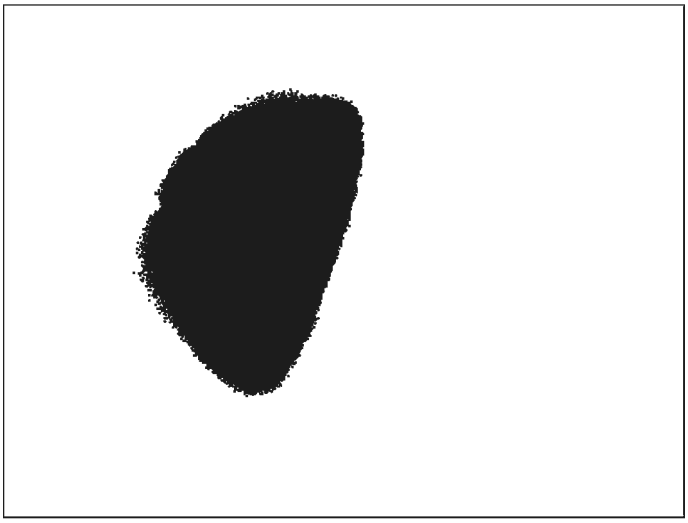

Fig. 5. The lens calculated on the basis of masks from Fig. 4.

3.2. SPOT ON THE LENS REGION DESCRIPTION

The spot on the lens is a region on the image which intensity is slightly darker when compared to the neighborhood. The intensity difference in this region not only is very small, but also it is connected with optical illusion. It means, that the spot shades are changing within the area, but the difference with neighborhood is constant and therefore it seems as the spot has constant colour. Taking this into consideration the method used to find this region is not fully automatic.

In order to determine the spot position the following techniques of image processing were applied. Firstly, there are considered only images in range 7-21, as the spot is invisible in other spectra. The chosen images $I(x,y)$ are processed with median filter M_F following the formula:

$$I_{proc}(x,y) = M_F(I(x \pm k, y \pm k)); \quad (2)$$

where k was set to 5. The aim of this step is to remove noises from the data. Next, the average image is calculated as:

$$I_{avg} = \frac{1}{N-7}\sum_{i=7}^{N} I_i(x,y)_{proc} \quad (3)$$

Finally, the thresholding operator is applied. According to performed experiment values 179 and 180 define the silhouette of the spot. Unfortunately, this values define additional outline in the image, therefore manual support is necessary to choose one of the defined lines. Fig. 6. presents the result before manual processing.

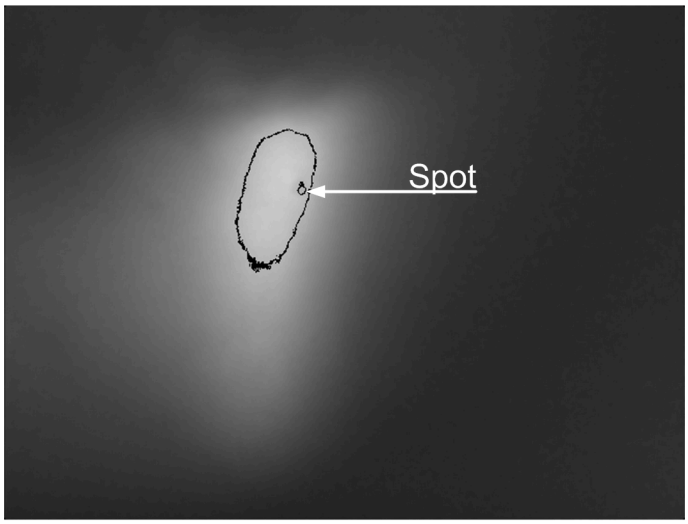

Fig. 6. The spot region defined automatically.

3.3. LINES CORRESPONDING TO VEINS

Finding the veins in the image is not a trivial task. The veins are visible only in few images, and only these are considered for calculation.

However, the vein seems to be easily distinguishable from the background, because it has darker intensity. It proved to be also an optical illusion, and when one tries to apply any thresholding or edge detection filter the lines are disappearing. It was found out, that the background as well as the vein in the image change its values gradually, keeping the difference between the object and background shades rather constant.

In presented approach firstly the algorithm concentrates on veins region estimation in each from multispectral images. Here, the median filter is used and followed by the adaptive thresholding. This method of veins detection has the following parameters:

- μ - the size of the median filter mask ($\mu \times \mu$),
- w - the size of the adaptive thresholding mask ($w \times w$),
- C - the subtracted constant in the adaptive thresholding.

It makes it easier to write the complete transformation with the helping variable k that is the half-width of the mask: $k_\mu = (\mu - 1)/2$ and $k_w = (w-1)/2$. The described steps of the image transformation are described with the following formulas:

$$I_{temp}(x,y) = M_F(I(x \pm k_\mu, y \pm k_\mu)) \tag{4}$$

$$I_{thresh}(x,y) = \left(\frac{1}{w^2} \sum_{i=-k_w}^{k_w} \sum_{j=-k_w}^{k_w} I_{temp}(x+i, y+j) \right) - I_{temp}(x,y) - C \tag{5}$$

$$I_{out}(x,y) = \begin{cases} 1 & I_{thresh}(x,y) \geq 0 \\ 0 & I_{thresh}(x,y) < 0 \end{cases} \tag{6}$$

The result of multispectral image processing for the purpose of veins detection is presented in the Fig. 7. There are also presented only components from 2 to 21.

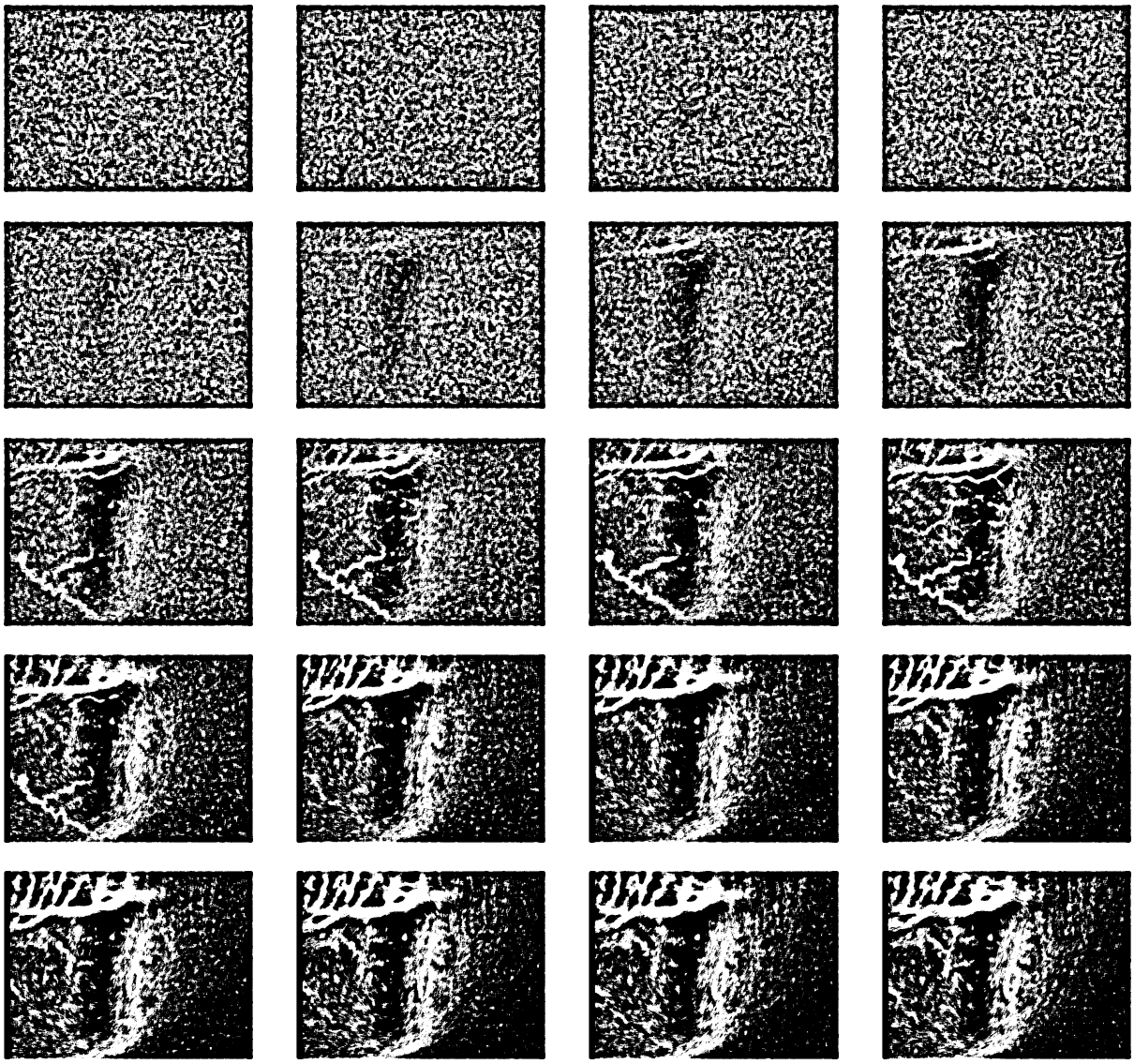

Fig. 7. Veins detection in 20 from 21 multispectral image components.

The suggested image transformation proved that it is possible to detect eyelashes and veins in multispectral images. It is noticed that veins are visible in images 10 – 15, whereas eyelashes are present in images 9 – 21. Unfortunately, it was impossible to exploit this knowledge for automatic system for vein detection.

4. CONCLUSIONS

In this paper the approach to select the most important parts of human eye parts from the multispectral images was presented. The original data contained 21 channel images: from 410 nm to 710 nm with the step of 15 nm. The efforts focused on defining several models of analysis that could select the following parts of the eye: lens, spot, and veins. For the first two objects it occurred to be possible to define the model of multispectral image processing that points regions of interests. Unfortunately, it was not possible to achieve the success in detection of veins. In this case only the most important components of multispectral image (from 545 nm to 605 nm) where veins are the most visible can be pointed out. It also occurred that the similar in shape - the eyelash - is visible in the wider spectrum: from the 545 nm up to 710 nm what may be useful in the further data analysis.

5. ACKNOWLEDGMENTS

This work was supported by the European Union from the European Social Fund (grant agreement number: UDA-POKL.04.01.01-00-106/09).

BIBLIOGRAPHY

[1] CAMPS-VALLS G., BRUZZONE L., Kernel-based methods for hyperspectral image classification, IEEE Transactions on Geoscience and Remote Sensing, 2005, Vol. 43, No. 6, pp. 1351–1362.
[2] DERRODE S., MERCIER G., PIECZYNSKI W., Unsupervised multicomponent image segmentation combining a vectorial HMC model and ICA, Int. Conf. on Image Processing, 2003, pp. 407–410.
[3] GAT N., Imaging spectroscopy using tunable filters: a review, Proceedings of SPIE - International Society for Optical Engineering, 2000, Vol. 4056, pp. 50–64.
[4] LAU D., VILLIS C., FURMAN S., LIVETT M., Multispectral and hyperspectral image analysis of elemental and micro-raman maps of cross-sections from a 16th century painting, Analytica Chimica Acta, 2008, Vol. 610, No. 1, pp. 15–24.
[5] MASOOD K., RAJPOOT N.M., Spatial analysis for colon biopsy classification from hyperspectral, Annals of the BMVA, 2008, Vol. 4, pp. 1–15.
[6] MERCIER G., DERRODE S., LENNON M., Hyperspectral image segmentation with markov chain model, In IEEE International Geoscience and Remote Sensing Symposium, 2003, pp. 3766 – 3768.
[7] MICHALAK M., ŚWITOŃSKI A., Spectrum evaluation on multispectral images by machine learning techniques, Lecture Notes in Computer Science, 2010, Vol. 6375, pp. 26–133.
[8] MICHALAK M., ŚWITOŃSKI A., Kernel postprocessing of multispectral images, Advances in Intelligent and Soft Computing, 2011, Vol. 95, pp. 395–401.
[9] MICHALAK M., ŚWITOŃSKI A., STAWARZ M., Selection of the most important components from multispectral images for detection of tumor tissue, Journal of Medical Informatics and Technologies, 2011, Vol. 17, pp. 303-307.
[10] RAJPOOT K., RAJPOOT N., SVM optimization for hyperspectral colon tissue cell classification, Lecture Notes in Computer Science, 2004, Vol. 3217, pp. 829–837.
[11] ŚWITOŃSKI A., BŁACHOWICZ T., ZIELIŃSKI M., MISIUK-HOJTO M., WOJCIECHOWSKI K., Ophthalmic diagnosis based on multispectral imaging, Electrical Review, 2011, Vol. 12B, pp. 165–168.
[12] ŚWITOŃSKI A., MICHALAK M., JOSIŃSKI H., WOJCIECHOWSKI K., Detection of tumor tissue based on the multispectral imaging, Lecture Notes in Computer Science, 2010, Vol. 6375, pp. 325-333.